TECHNISCHE MECHANIK, Band 25, Heft 1, (2005), 27-38
Manuskripteingang: 27. Mai 2004

Neural Signals of Nonlinear Conical Nozzles

W. K. Chai, J. G. DeHaven, M. Hanson, H. S. Tzou

Conventional sensors, such as proximeters and accelerometers, are add-on devices usually adding additional weights to structures and machines. Health monitoring of flexible structures by electroactive smart materials has been investigated over the years. Thin-film piezoelectric material, e.g., polyvinylidene fluoride (PVDF) polymeric material, is a lightweight and dynamic sensitive material appearing to be a perfect candidate in monitoring structure's dynamic state and health status of flexible shell structures with complex geometries. The complexity of shell structures has thwarted the progress in studying the distributed sensing of shell structures. Linear distributed sensing of various structures have been studied, e.g., beams, plates, cylindrical shells, conical shells, spherical shells, paraboloidal shells and toroidal shells. However, distributed microscopic neural signals of nonlinear shell structures have not been carried out rigorously. This study is to evaluate microscopic signals, modal voltages and distributed micro-neural signal components of truncated nonlinear conical shells laminated with distributed infinitesimal piezoelectric neurons. Signal generation of distributed neuron sensors laminated on conical shells is defined first. The dynamic neural signal of truncated nonlinear conical shells consists of microscopic linear and nonlinear membrane components and linear bending component based on the von Karman geometric nonlinearity. Micro-signals, modal voltages and distributed neural signal components of a truncated nonlinear conical shell are investigated and their sensitivities discussed.

1 Introduction

Typical off-the-shelf sensors to be added at discrete locations within a system are not always the best method for monitoring the health of today's complex precision designed machines and structures. While many common types of these "discrete" sensors, such as proximeters, LVDT, and accelerometers, are readily available with their specifications and limitations included, they typically add weight and do not always measure the true system response since their presence may affect the system's behavior. In comparison, thin-film piezoelectric material, e.g., polyvinylidene fluoride (PVDF) polymeric material, is a lightweight and dynamic sensitive material and it can be easily segmented and shaped to account for various in-situ distributed monitoring applications of flexible structures (Gabbert and Tzou, 2001; Tzou and Anderson, 1992). Unlike conventional discrete add-on sensors, thin piezoelectric layers can be spatially spread and distributed over the surfaces of precision structures. Accordingly, these distributed piezoelectric layers can serve as distributed neurons and actuators in sensing and control of advanced structures and machines (Howard et al., 2001; Howard, 1991; Tzou, 1993). One possible application is the housing for optical instruments. Whether trying to capture light from a distant galaxy to form a clear image of the positions and numbers of stars or creating a high powered beam for a particular laser, unwanted vibration can be a problem when precision is extremely important for such devices (Tyson, 1998). To minimize the effects from many possible sources of disturbances which can lead to vibration, the housing needs to damp out the vibration before it reaches the lenses. Depending on the application and desired configuration, the housing structure will most likely be some form of shell, possibly a cylindrical shell or even a shallow conical shell. Dynamics and vibrations of conical shell structures have been investigated over the years (Hu, 1964; Platus, 1965; Newton, 1966; Hu et al., 1966; Krause, 1968; Bazhenov and Igonicheva, 1987; Wang and To, 1991; Lim and Liew, 1996; Tong, 1996; Xu et al., 1996). Distributed sensing characteristics of rings, cylindrical shells, toroidal shells, paraboloidal shells, etc. have been evaluated (Tzou et al., 1993; Tzou et al., 1996; Tzou and Wang, 2002; Tzou and Ding, 2004; Ding and Tzou, 2004; Tzou, 1992). However, distributed sensing and control of conical shells have not been thoroughly investigated. Dynamic sensing characteristics, micro-signal generations, and distributed modal voltages of truncated linear conical shell sections have been evaluated recently (Tzou et al., 2003). This study is to investigate microscopic signal generations and neural spatial distributed modal signals of nonlinear conical shells based on infinitesimal piezoelectric neurons.

Signal generation of distributed neuron sensors laminated on nonlinear conical shells is defined first. Closed-form sensing signal generation of distributed conical shell sensors is then defined based on given boundary conditions and mode shape functions following the Donnell-Mushtari-Vlasov theory. Micro-signals, modal

voltages and distributed sensing components of a free-free truncated nonlinear conical shell are investigated and their sensitivities discussed in a case study.

2 Distributed Sensing of Nonlinear Shells

The generic shell sensing signal equation is derived based on the direct piezoelectric effect, the Gauss theory, the open circuit assumption, the Maxwell equation, and also the generic double curvature shell theory. In general, in-plane strains S_{ij}^s in the neural sensor layer contribute to the signal generation ϕ^s:

$$\phi^s = \frac{h^s}{S^e} \int_{\alpha_1} \int_{\alpha_2} \left(h_{31} S_{11}^s + h_{32} S_{22}^s + h_{36} S_{12}^s \right) A_1 A_2 d\alpha_1 d\alpha_2 \,, \tag{1}$$

where h^s is the thickness of the sensor layer; the superscript 's' denotes the distributed sensor layer; S^e is the effective electrode area of the sensor layer. α_1 and α_2 are the two principal directions in generic shell continuum; A_1 and A_2 are the Lamé parameters; and h_{31}, h_{32} and h_{36} are the piezoelectric constants. The effect of transverse strains S_{13}, S_{23} and S_{33} are neglected, since the variation is small in the α_3 direction, provided the shell and the sensor are thin. Moreover, the sensor material is assume to be insensitive to the in-plane twisting S_{12}^s. eq.(1) becomes

$$\phi^s = \frac{h^s}{S^e} \int_{x} \int_{\psi} \left(h_{31} S_{xx}^s + h_{32} S_{\psi\psi}^s \right) \bullet x \sin\beta^* \, dx d\psi \tag{2}$$

The strain terms can be written as the summation of the membrane strain s_{ij}^o and the bending strain k_{ij}: $S_{xx}^s = s_{xx}^o + r_x^s k_{xx}$ and $S_{\psi\psi}^s = s_{\psi\psi}^o + r_\psi^s k_{\psi\psi}$. The large deformation effect takes place in the membrane strains only, the membrane strains of the nonlinear conical shell are defined as

$$s_{xx}^o = \frac{\partial u_x}{\partial x} + \frac{1}{2}\left(\frac{\partial u_3}{\partial x} \right)^2 \tag{3a}$$

$$s_{\psi\psi}^o = \frac{1}{x \sin\beta^*} \frac{\partial u_\psi}{\partial \psi} + \frac{u_x}{x} - \frac{u_3}{x \tan\beta^*} + \frac{1}{2} \frac{1}{x \sin\beta^*} \left(\frac{\partial u_3}{\partial \psi} \right)^2 \tag{3b}$$

Furthermore, in-plane displacements u_x and u_ψ are neglected in bending strains based on the Donnell-Mushtari-Vlasov theory. Thus, the bending strains of the conical shell are

$$k_{xx} = -\frac{\partial^2 u_3}{\partial x^2} \text{ and } k_{\psi\psi} = -\frac{1}{x^2 \sin^2\beta^*} \frac{\partial^2 u_3}{\partial \psi^2} - \frac{1}{x} \frac{\partial u_3}{\partial x} \tag{4a,b}$$

A generic sensing signal equation with explicit displacement expression is derived by substituting the membrane strains and bending strains into eq.(1).

3 Nonlinear Conical Shell Sensing Equation

Note that the generic sensing equation can account for both the linear and nonlinear effects. Moreover, the strain terms in the sensing signal equation can be divided into the membrane strains and the bending strains. Thus, the signal generation of a generic shell sensor layer laminated on an elastic thin shell with the von-Karman geometric nonlinearity becomes

$$
\begin{aligned}
\phi^s = \left(\frac{h^s}{S^e}\right)\int_{\alpha_1}\int_{\alpha_2} \Bigg\{ & h_{31}\Bigg\{\Bigg(\frac{1}{A_1}\frac{\partial u_1}{\partial \alpha_1} + \frac{u_2}{A_1 A_2}\frac{\partial A_1}{\partial \alpha_2} + \frac{u_3}{R_1} + \left[\frac{1}{2}\left(\frac{\partial u_3/\partial \alpha_1}{A_1}\right)^2\right]\Bigg) \\
& + r_1^s\left[\frac{1}{A_1}\frac{\partial}{\partial \alpha_1}\left(\frac{u_1}{R_1} - \frac{1}{A_1}\frac{\partial u_3}{\partial \alpha_1}\right) + \frac{1}{A_1 A_2}\left(\frac{u_2}{R_2} - \frac{1}{A_2}\frac{\partial u_3}{\partial \alpha_2}\right)\frac{\partial A_1}{\partial \alpha_2}\right]\Bigg\} \\
& + h_{32}\Bigg\{\Bigg(\frac{1}{A_2}\frac{\partial u_2}{\partial \alpha_2} + \frac{u_1}{A_1 A_2}\frac{\partial A_2}{\partial \alpha_1} + \frac{u_3}{R_2} + \left[\frac{1}{2}\left(\frac{\partial u_3/\partial \alpha_2}{A_2}\right)^2\right]\Bigg) \\
& + r_2^s\left[\frac{1}{A_2}\frac{\partial}{\partial \alpha_2}\left(\frac{u_2}{R_2} - \frac{1}{A_2}\frac{\partial u_3}{\partial \alpha_2}\right) + \frac{1}{A_1 A_2}\left(\frac{u_1}{R_1} - \frac{1}{A_1}\frac{\partial u_3}{\partial \alpha_1}\right)\frac{\partial A_2}{\partial \alpha_1}\right]\Bigg\} \\
& + h_{36}\Bigg\{\Bigg(\frac{1}{A_2}\frac{\partial u_1}{\partial \alpha_2} + \frac{1}{A_1}\frac{\partial u_2}{\partial \alpha_1} - \frac{u_1}{A_1 A_2}\frac{\partial A_1}{\partial \alpha_2} - \frac{u_2}{A_1 A_2}\frac{\partial A_2}{\partial \alpha_1} + \left[\frac{1}{A_1 A_2}\frac{\partial u_3}{\partial \alpha_1}\frac{\partial u_3}{\partial \alpha_2}\right]\Bigg) \\
& + r_{12}^s\left[\frac{A_1}{A_2}\frac{\partial}{\partial \alpha_2}\left(\frac{u_1}{R_1} - \frac{1}{A_1}\frac{\partial u_3}{\partial \alpha_1}\right)\frac{1}{A_1} + \frac{A_2}{A_1}\frac{\partial}{\partial \alpha_1}\left(\frac{u_2}{R_2} - \frac{1}{A_2}\frac{\partial u_3}{\partial \alpha_2}\right)\frac{1}{A_2}\right. \\
& \left. - \frac{1}{A_1 A_2}\left(\frac{u_1}{R_1} - \frac{1}{A_1}\frac{\partial u_3}{\partial \alpha_1}\right)\frac{\partial A_1}{\partial \alpha_2} - \frac{1}{A_1 A_2}\left(\frac{u_2}{R_2} - \frac{1}{A_2}\frac{\partial u_3}{\partial \alpha_2}\right)\frac{\partial A_2}{\partial \alpha_1}\right]\Bigg\}\Bigg\} \bullet A_1 A_2 d\alpha_1 d\alpha_2
\end{aligned}
\tag{5}
$$

where A_i is the Lamé parameter; R_i is the radius of curvature of the α_i axis; u_i is the displacement in the α_i direction; r_i^s denotes the sensor location away from the shell neutral surface; the terms inside the parentheses following the piezoelectric constant denote the membrane strain; the terms with r_i^s are the bending strains; and the quadratic terms in the membrane strains are the large deformation effect based on the von Karman geometric nonlinearity (Tzou and Yang, 2000). Application of the generic sensing equation depends on two Lamé parameters, two radii of curvatures and two principal direction of a given geometry. Figure 1 illustrates a conical shell and its parameters. The Lamé parameters, radii of curvature, and principal directions of conical shells are respectively defined by $A_1 = 1$, $A_2 = x\sin\beta^*$, $R_1 = R_x = \infty$, $R_2 = R_\psi = x\tan\beta^*$, $\alpha_1 = x$, and $\alpha_2 = \psi$. β^* is the half-apex angle; x is the distance measured from the apex. Note that the Donnell-Mushtari-Vlasov theory is used and micro-signal generations of a free-free truncated nonlinear conical shell are investigated in this study.

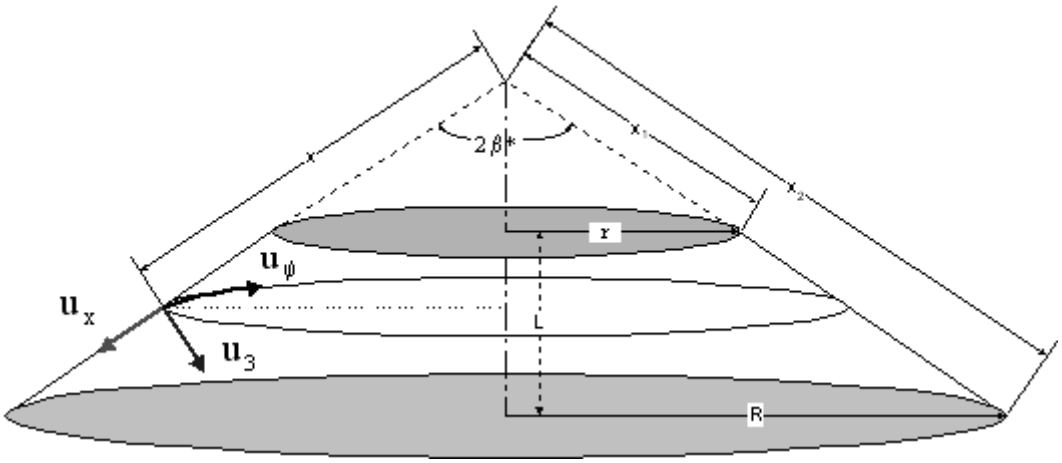

Figure 1. A conical shell of revolution

Thus, according to eq.(5) and with neglected in-plane twisting S_{12}^s, the sensing signal equation of a distributed neural sensor laminated on a nonlinear conical shell becomes

$$\begin{aligned}\phi^s = &\left(\frac{h^s}{S^e}\right)\int_x \int_\psi \left\{h_{31}\left\{\frac{\partial u_x}{\partial x}+\frac{1}{2}\left(\frac{\partial u_3}{\partial x}\right)^2 - r_x^s\frac{\partial^2 u_3}{\partial x^2}\right\}\right. \\ &+h_{32}\left\{\frac{1}{x\sin\beta^*}\frac{\partial u_\psi}{\partial\psi}+\frac{u_x}{x}-\frac{u_3}{x\tan\beta^*}+\frac{1}{2}\frac{1}{x\sin\beta^*}\left(\frac{\partial u_3}{\partial\psi}\right)^2\right. \\ &\left.\left.+r_\psi^s\left[-\frac{1}{x^2\sin^2\beta^*}\frac{\partial^2 u_3}{\partial\psi^2}-\frac{1}{x}\frac{\partial u_3}{\partial x}\right]\right\}\right\} \bullet x\sin\beta^* dx\,d\psi\end{aligned} \tag{6}$$

Boundary shear forces and moments are zero for free-free boundaries conditions, i.e., $N_{xx}=N_{xx}^*=0$ at $x=x_1$ and x_2 and $N_{x\psi}=N_{x\psi}^*=0$ at $x=x_1$ and x_2. Thus,

$$\begin{aligned}\frac{1}{x}\left[\frac{\partial}{\partial x}(xM_{xx})-M_{\psi\psi}-2\frac{\partial M_{x\psi}}{\partial\psi}\csc\beta^*\right] &= \frac{1}{x}\left[xQ^*_{xx}-\csc\beta^*\frac{\partial M^*_{x\psi}}{\partial\psi}\right] \\ &= 0 \quad \text{at } x=x_1 \text{ and } x=x_2\end{aligned} \tag{7}$$

$$M_{xx}=M^*_{xx}=0 \quad \text{at } x=x_1 \text{ and } x_2 \tag{8}$$

Accordingly, the assumed displacement solutions for a free-free truncated conical shell are

$$u_x = U_{xm}(x)\cos m\psi\sin\omega t\,,\quad u_\psi = U_{\psi m}(x)\sin m\psi\sin\omega t\,,\quad u_3 = U_{3m}(x)\cos m\psi\sin\omega t\,, \tag{9a,b,c}$$

$U_{xm}(x)\cos m\psi$ denotes the longitudinal mode shape function; $U_{\psi m}(x)\sin m\psi$ denotes the circumferential mode shape function; and $U_{3m}(x)\cos m\psi$ denotes the transverse mode shape function, where $U_{xm}(x)$, $U_{\psi m}(x)$ and $U_{3m}(x)$ are the longitudinal displacement functions defined as functions of x and they can be specified depending on accuracy requirement (Platus, 1965); m is the (circumferential) wave number. In free vibration analysis, the longitudinal displacement function is chosen to be $(x/x_2)^p$ where p is the power of the polynomial function that can be regarded as the wave number in the longitudinal direction; x_2 is the (longitudinal) length from the apex to the bottom perimeter. Higher-order polynomial function of $U_{xm}(x)$, $U_{\psi m}(x)$ and $U_{3m}(x)$, i.e., more flexible, can improve the accuracy of the free vibration analysis, especially for higher natural modes at higher natural frequencies. The power p of the longitudinal mode shape polynomial function selected in this analysis is based on a free vibration analysis evaluated previously (Platus, 1965). Note that the microscopic signal analysis is to reveal the modal signals corresponding to spatially distributed microscopic directional strains generated by free vibrations. Accordingly, one can infer that precise free-vibration analysis leads to better strain prediction resulting in accurate modal signal prediction and vibration diagnosis. Based on this analysis, one can easily utilize piezoelectric neurons placed at optimal locations and directions to diagnose shell dynamic states. Substituting mode shape functions and taking derivatives with respect to ψ, one can derive the sensing signal generation of a free-free truncated nonlinear conical shell.

$$\begin{aligned}\phi^s = &\left(\frac{h^s}{S^e}\right)\int_x \int_\psi \left\{h_{31}\left[\frac{\partial U_{xm}(x)\cos m\psi}{\partial x}+\frac{1}{2}\left(\frac{\partial U_{3m}(x)}{\partial x}\right)^2(\cos m\psi)^2 + r_x^s\left(-\frac{\partial^2 U_{3m}(x)\cos m\psi}{\partial x^2}\right)\right]\right. \\ &+h_{32}\left[\frac{m\cdot U\psi m(x)\cos m\psi}{x\sin\beta^*}+\frac{U_{xm}(x)\cos m\psi}{x}-\frac{U_{3m}(x)\cos m\psi}{x\tan\beta^*}+\frac{1}{2}\frac{1}{x^2\sin\beta^*}\left(\frac{\partial U_{3m}(x)}{\partial x}\right)^2\right. \\ &\left.\left.(\cos m\psi)^2+r_\psi^s\left(\frac{m^2 U_{3m}(x)\cos m\psi}{x^2\sin^2\beta^*}-\frac{1}{x}\frac{\partial U_{3m}(x)\cos m\psi}{\partial x}\right)\right]\right\}\cdot x\sin\beta^* dx d\psi.\end{aligned} \tag{10}$$

Furthermore, using the generic displacement function $(x/x_2)^p$ with $p = 1$ and taking derivatives with respect to x yields the signal generation of the first mode group (1,m) of truncated nonlinear conical shells.

$$\phi^s = \left(\frac{h^s}{S^e}\right)\int_x \int_\psi h_{31}\left\{\left[\frac{\cos m\psi}{x_2}+\frac{1}{2}\frac{(\cos m\psi)^2}{{x_2}^2}\right]+h_{32}\left[\frac{m\cdot\cos m\psi}{x_2\sin\beta^*}+\frac{\cos m\psi}{x_2}-\frac{\cos m\psi}{x_2\tan\beta^*}\right.\right.$$
$$\left.\left.+\frac{1}{2}\frac{1}{(x\sin\beta^*)^2}\frac{(\cos m\psi)^2}{{x_2}^2}+r_\psi^s\left(\frac{m^2\cos m\psi}{x\,x_2\sin^2\beta^*}-\frac{1}{x}\frac{\cos m\psi}{x_2}\right)\right]\right\}\cdot x\sin\beta^* dx d\psi\,. \tag{11}$$

Following the same procedures and using p=2 yields the signal generation of the second mode group (2,m) of truncated nonlinear conical shells.

$$\phi^s = \left(\frac{h^s}{S^e}\right)\int_x \int_\psi \left\{h_{31}\left[2\cos m\psi\frac{x}{x_2^2}[1+\frac{x}{x_2^2}\cos m\psi]+r_x^s\left(-2\cos m\psi\frac{1}{x_2^2}\right)\right]\right.$$
$$+h_{32}\left[\frac{x}{x_2^2}(1+\frac{m}{\sin\beta^*}-\frac{1}{\tan\beta^*}+\frac{1}{x\sin\beta^*}\frac{2}{x_2^2}\cos m\psi)\cos m\psi\right. \tag{12}$$
$$\left.\left.+r_\psi^s(\frac{1}{x_2^2}\cos m\psi(\frac{m^2}{\sin^2\beta^*}-2))\right]\right\}\cdot x\sin\beta^* dx\,d\psi\,.$$

Note that the above sensing signal is defined for a distributed sensor neuron with an effective electrode area S^e. Removing the surface integration and dropping the surface average yields a microscopic signal component of an infinitesimal sensor neuron. Detailed spatial distribution of local micro-signals (i.e., the distributed *modal voltages*) can be established and spatially distributed modal sensing characteristics can be evaluated. For higher mode groups of nonlinear truncated conical shells, one can assign p=n and follow the same procedures to define explicit signal generations.

4 Evaluation of Micro-Signal Generation and Distribution

Micro-signal generations and spatially distributed neural signals of a nonlinear truncated conical shell of revolution are investigated in this section. Dimensions for the conical shell model used in the case study are listed in Table 1, also refer to Figure 1. Spatial signal distributions of two mode groups (p=1,2) and four natural modes (m=2,3,4,5) of the model are evaluated and detailed micro-signal contributions are compared and analyzed. (Note that the m=1 mode is a rigid-body mode. Hence, there is no signal generation.)

	Geometry
Conical Shell Half-Apex Angle β^*	60.42^o
Major Radius, R	10.00 in
Minor Radius, r	4.45 in
Length, L	3.15 in
Thickness, h	0.01 in

Table 1. Definitions of the two conical shell models

The First Mode Group (1,*m*=2-5)

Distributed micro-signal components and modal neural voltages of the first mode group (1,*m*=2-5) are presented in Figures 2-5. The top-left signal distribution denotes the signal component resulting from the longitudinal membrane strain; the top-right signal denotes the signal component resulting from the circumferential membrane strain; the bottom-left signal denotes the signal component resulting from the circumferential bending strain; and the bottom-right denotes the overall signal distribution – *the (k,m)-th modal voltage*, including all contributing micro-signal components. Note that the longitudinal bending strain (k_{xx}) signal vanishes due to the selected displacement function with p=1. The wire-frame illustrates the spatially distributed signals superimposed on the shaded conical shell model.

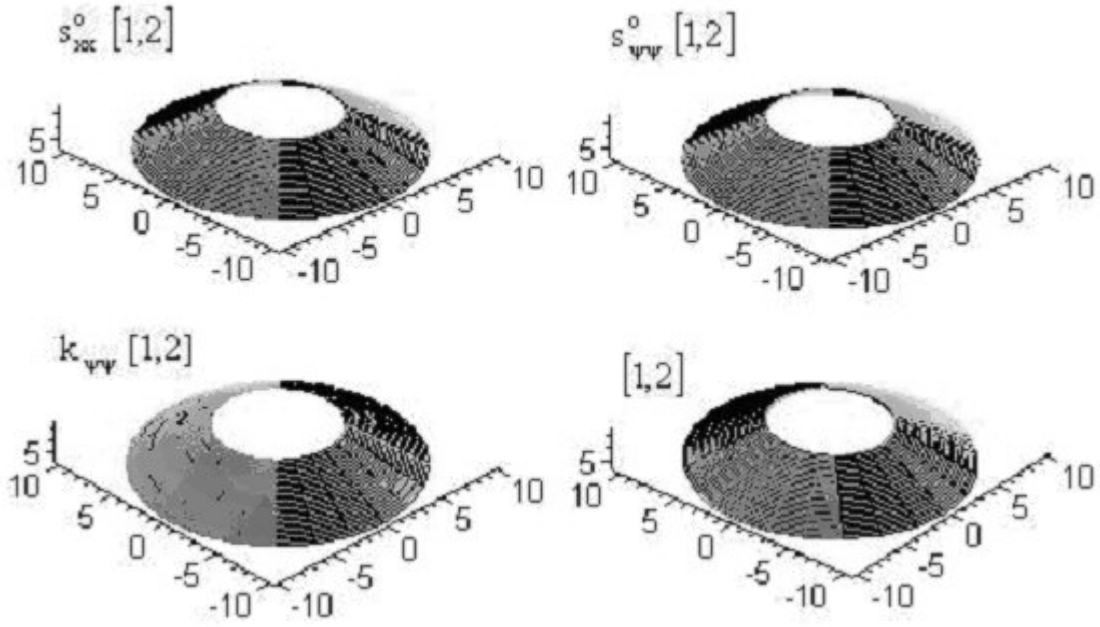

Figure 2. Signal components and modal voltage of (1,2) mode

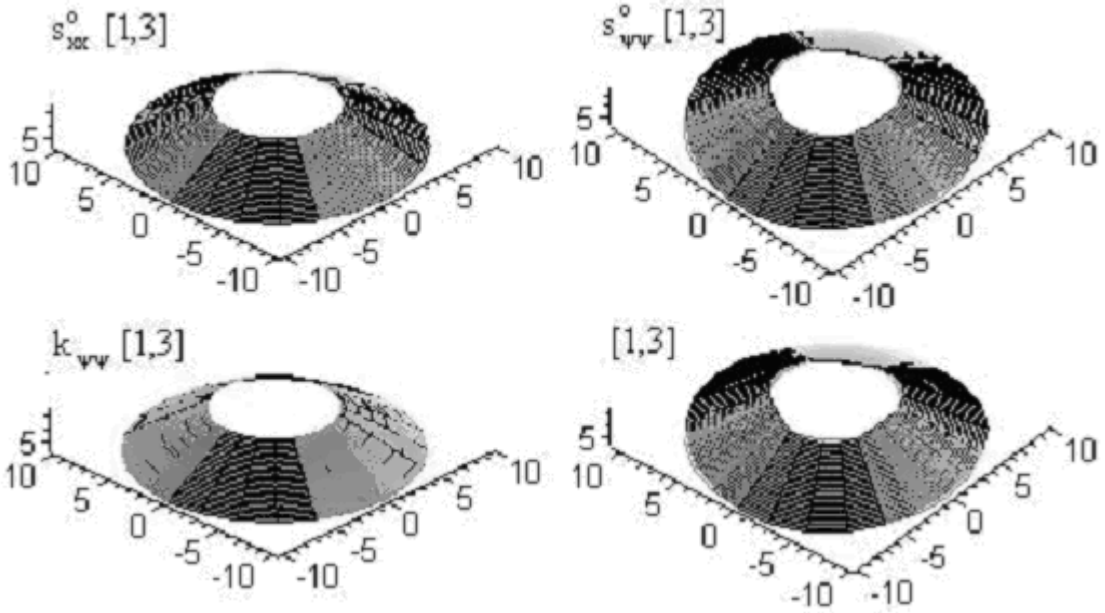

Figure 3. Signal components and modal voltage of (1,3) mode

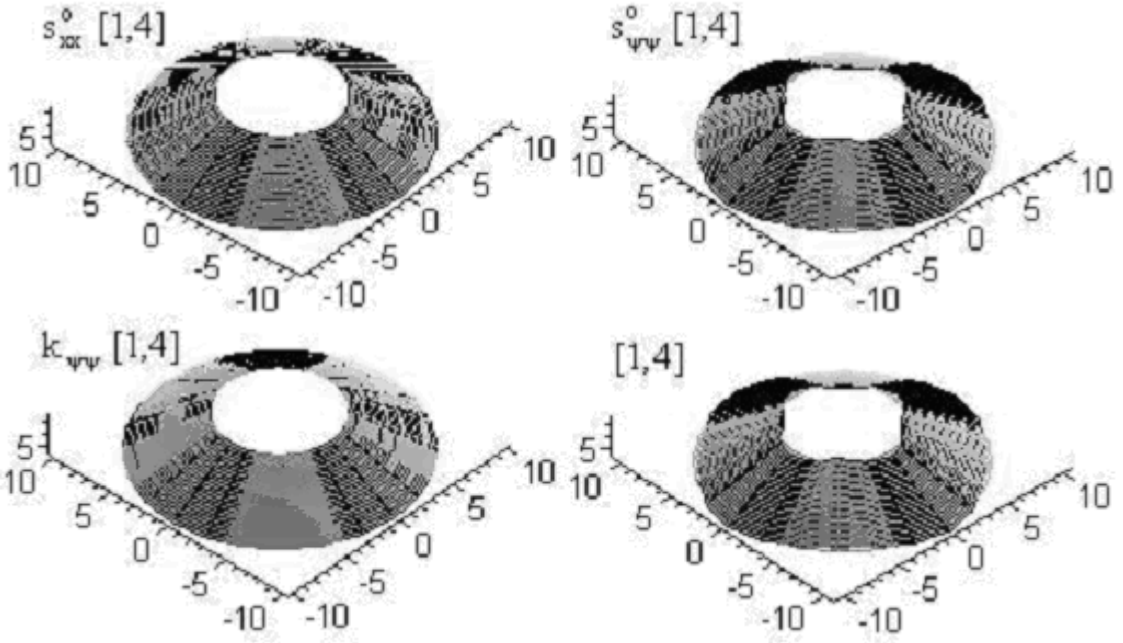

Figure 4. Signal components and modal voltage of (1,4) mode

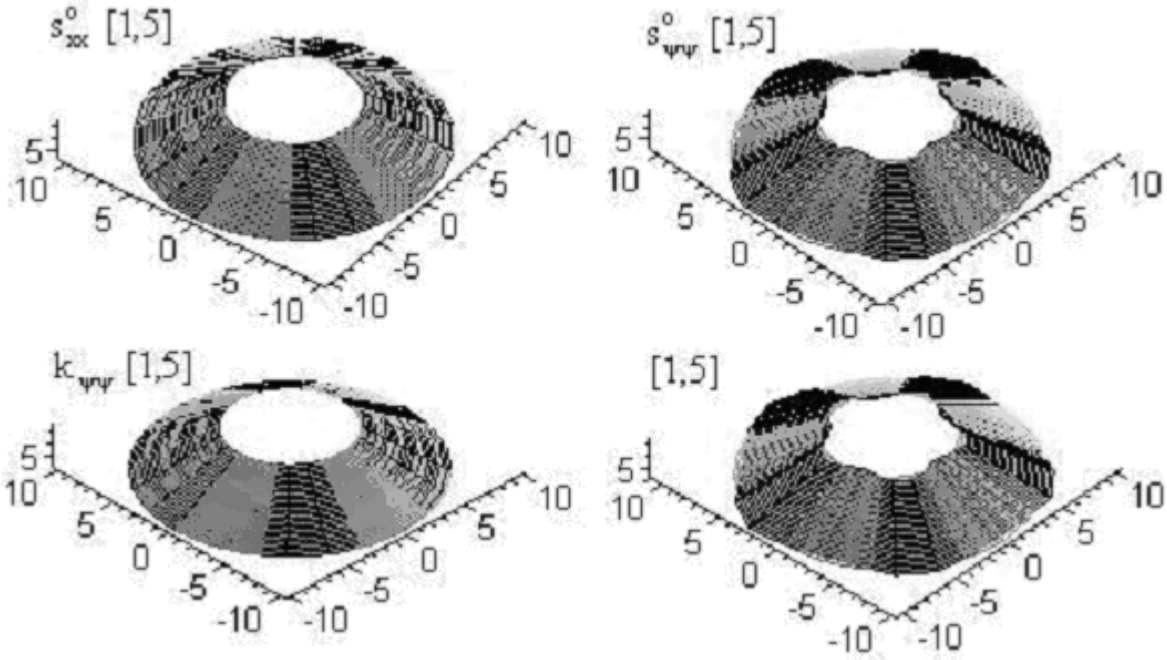

Figure 5. Signal components and modal voltage of (1,5) mode

The Second Mode Group (2, *m*=2-5)

Distributed micro-signal components and modal voltages of the second mode group (2, *m*=2-5) are presented in Figures 6-9. The top-left signal distribution denotes the signal component resulting from the longitudinal membrane strain; the top-right signal denotes the signal component resulting from the circumferential membrane strain; the middle-left signal denotes the signal component resulting from the longitudinal bending strain; the middle-right signal denotes the signal component resulting from the circumferential bending strain; and the bottom-left denotes the overall signal distribution – *the (k,m)-th modal voltage*, including all contributing signal components. Note that the longitudinal bending strain exists in this case, with the displacement function *p*=2. Note that the spatially distributed signal generations basically exhibit distinct modal characteristics and the spatially distributed signal patterns – *the modal voltages* - clearly reveal the distinct modal dynamic and micro-strain characteristics of conical shells. (Usually, high strain regions result in high signal magnitudes.) Observing these micro-neural signal components (i.e., the longitudinal/circumferential membrane components and the longitudinal/circumferential bending components) suggests that 1) the dominating micro-signal component among the four signal components is the circumferential membrane component, and 2) the micro-signals resulting from the nonlinear membrane strain is insignificant.

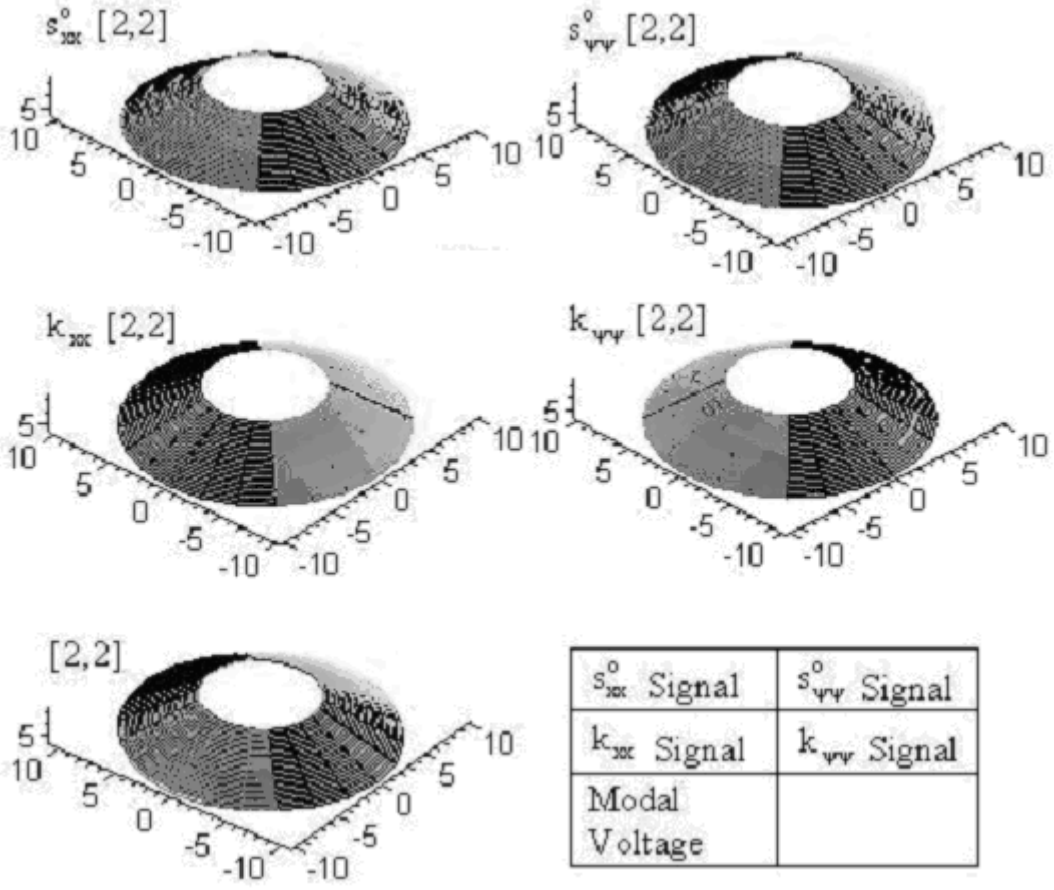

Figure 6. Signal components and modal voltage of (2,2) mode

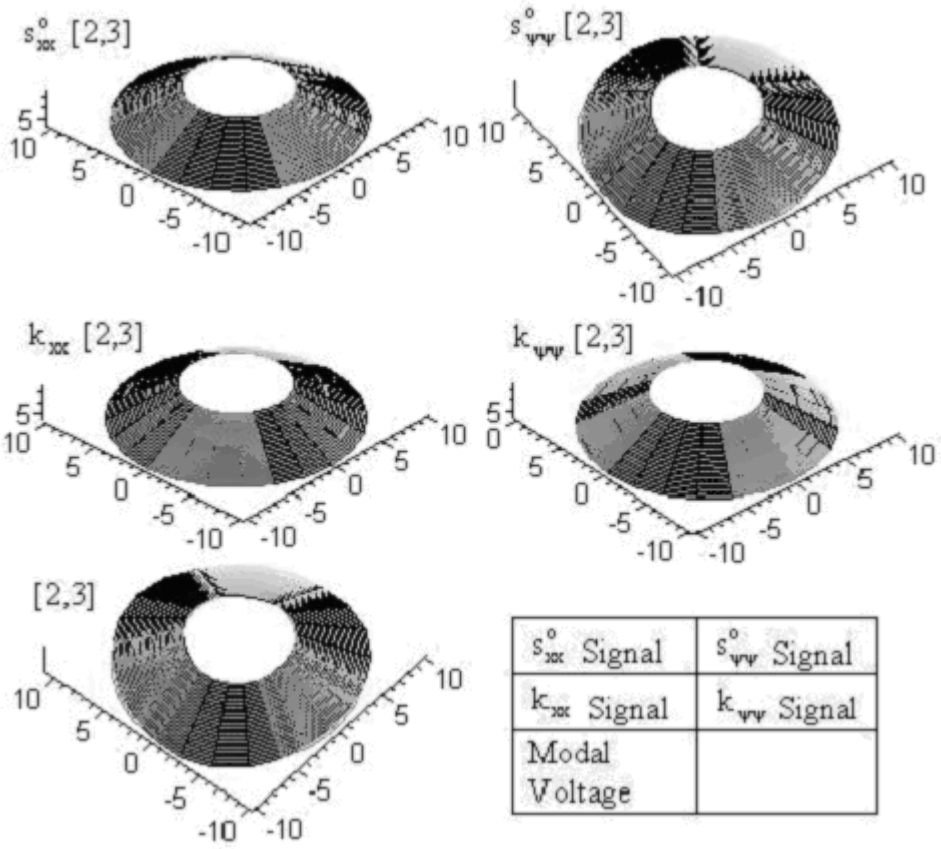

Figure 7. Signal components and modal voltage of (2,3) mode

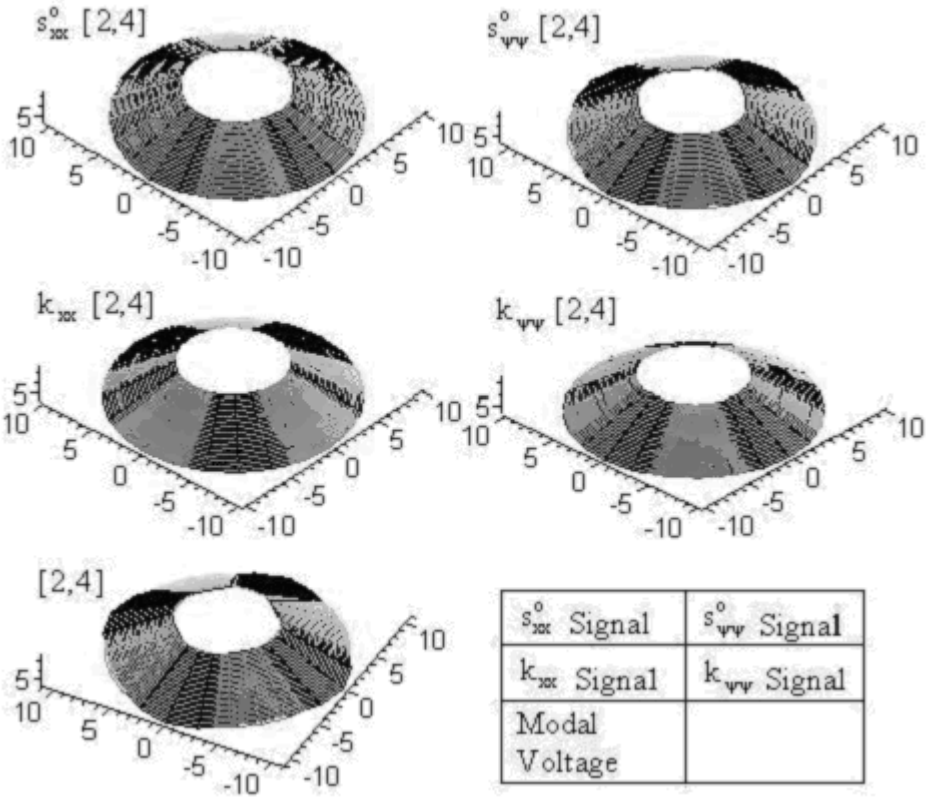

Figure 8. Signal components and modal voltage of (2,4) mode

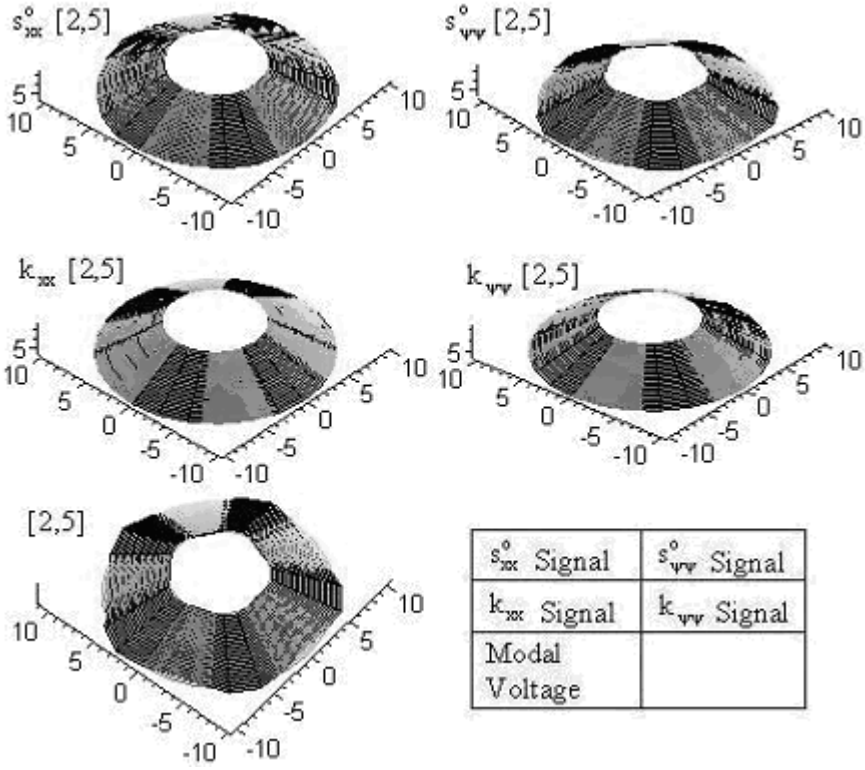

Figure 9. Signal components and modal voltage of (2,5) mode

5 Conclusions

Health monitoring and diagnosis is an important issue in modern high-performance precision structures and systems. Although dynamics and vibration of conical shell structures have been investigated over the years, distributed sensing and control of precision conical shells have not been thoroughly investigated. Conventional "discrete" add-on sensors, such as proximeters, LVDT, and accelerometers, usually add additional weights and often influence dynamic responses of precision structures and machines. However, unlike conventional discrete add-on sensors, thin-film piezoelectric layers are lightweight and they can be spatially spread and distributed over the surfaces of precision structures. Accordingly, these distributed piezoelectric layers can serve as distributed neurons and actuators in sensing and control of advanced structures and machines. Dynamic sensing characteristics, micro-signal generations, and distributed modal voltages of truncated nonlinear conical shell sections with infinitesimal piezoelectric neurons are investigated in this study. Signal generation of distributed neuron sensors laminated on nonlinear conical shells was defined first. Microscopic sensing signal generations for a free-free truncated nonlinear conical shell were defined based on the Donnell-Mushtari-Vlasov theory and assumed mode shape functions with a polynomial expression $(x/x_2)^p$ for the longitudinal waves and trigonometric (sine or cosine) expression for the circumferential waves.

Micro-neural signals, modal voltages and distributed sensing components of a free-free truncated nonlinear conical shell were investigated and their sensitivities discussed in case studies. Two mode groups (p=1,2) and four modal signals (m=2-5) of the conical shell model were calculated and plotted. Directional micro-signal components (i.e., the longitudinal membrane component, the circumferential membrane component, the longitudinal bending component, and the circumferential bending component) and spatially distributed modal voltages of the conical shell model were investigated. These microscopic signal generations reveal that the dominating signal component among the four contributing micro-signal components is the circumferential membrane component. Both geometry and boundary conditions influence modal characteristics, strain distributions, as well as signal generations. The spatially distributed neural signal patterns – *the modal voltages* - clearly represent the distinct modal dynamic characteristics and micro-strain variations of conical shells.

Acknowledgements

This research is supported, in part, by a grant from the NASA-Glenn Research Center. This support is gratefully acknowledged.

References

Bazhenov, V.G.; Igonicheva, V.: Nonlinear Analysis of Nonaxisymmetric Buckling of Cylindrical and Conical Shells in Axial Impact. *Prikladnaya Mekhanika*, 23, (1987), 10-17.

Ding, J.H.; Tzou, H.S.: Micro-electromechanics of Sensor Patches on Free Paraboloidal Shell Structronic Systems, *Mechanical Systems and Signal Processing*, 18, (2004), pp.367-380.

Gabbert, U.; Tzou, H.S.: Editors *Smart Structures and Structronic Systems* IUTAM. Symposium on Smart Structures and Structronic Systems, Kluwer Academic Publishers, Dordrecht/Boston/London (2001).

Howard, R.: *Piezothermoelasticity Applied to Distributed Sensing and Control* M.S. thesis, The University of Kentucky (1991).

Howard, R.; Chai, W.K.; Tzou, H.S.: Modal Voltages of linear and non linear Structures Using Distributed Artificial Neurons. *Mechanical Systems and Signal Processing* 15, (2001), 629-640.

Hu, W.C.L.: Free Vibration of Conical Shells. NASA Report TN D-2666, (1964).

Hu, W.C.L.; Gormley, J.F.; Lindholm, U.S.: Flexural Vibrations of Conical Shells with Free Edges. NASA Report CR 384, (1966).

Krause, F.A.: *Natural Frequencies and Mode Shapes of the Truncated Conical Shell with Free Edges* Ph.D. dissertation, The University of Arizona (1968).

Lim, C.W.; Liew, K.M.: Vibration of Shallow Conical Shells with Shear Flexibility: A First Order Theory. *Int. J. Solids Structures,* Vol.33, No. 4, (1996), pp.451-468.

Newton, R.A.: Free Vibrations of Rocket Nozzles. *AIAA J.* 4, (1966), 1303-1305.

Platus, D.H.: Conical Shell Vibrations. NASA Report TN D-2767, (1965).

Tong, L.: Effect of Axial Load on Free Vibration of Orthotropic Truncated Conical Shells. *Transaction of the ASME*, *Journal of Vibration & Acoustics* 118, (1996), 164-168.

Tyson, R.K.: *Principles of Adaptive Optics*. 2nd Ed. Academic Press, USA, (1998).

Tzou, H.S.: Thin-Layer Distributed Piezoelectric Neurons and Muscles: Electromechanics and Applications. *Precision Sensors, Actuators, and Systems*, H.S. Tzou and T. Fukuda, (Editors), Kluwer Academic Publishers, Dordrecht /Boston /London, (1992), 175-218.

Tzou, H.S.: *Piezoelectric Shells-Distributed Sensing and Control of Continua.* Kluwer Academic Publishers, Boston/Dordrecht (1993).

Tzou, H.S.; Anderson G.L.: Editors *Intelligent Structural Systems.* Kluwer Aca. Pub., Dordrecht/Boston (1992).

Tzou, H.S.; Ding, J.H.: Distributed Modal Voltages of Nonlinear Paraboloidal Shells with Distributed Neurons. *Journal of Vibration and Acoustics*. Vol.126, Jan. (2004). (Paper No. JVA 00-161)

Tzou, H.S.; Wang, D.W.: Micro-sensing Characteristics and Modal Voltages of Linear/nonlinear Toroidal Shell. *Journal of Sound and Vibration*, 254, (2002), 203-218.

Tzou, H.S.; Yang, R.J.: Nonlinear Piezo-thermoelastic Shell Theory applied to Control of Variable-geometry Shells. *Journal of Theoretical and Applied Mechanics* 38, (2000), 623-644.

Tzou, H.S.; Bao, Y.; Venkayya, V.B.: Study of Segmented Transducers Laminated on Cylindrical Shells, Part-1: Sensor Patches. *Journal of Sound & Vibration* 197, (1996), 207-224.

Tzou, H.S.; Chai, W.K.; Wang, D.W.: Modal Voltages and Micro-Signal Analysis of Conical Shells of Revolution. *Journal of Sound & Vibration* 260, (2003), 589-609.

Tzou, H.S.; Zhong, J.P.; Natori, M.C.: Sensor Mechanics of Distributed Shell Convolving Sensors Applied to Flexible Rings. *ASME Journal of Vibration & Acoustics* 115, (1993), 40-46.

Wang, B.; To, C.W.S.: Vibration Analysis of Truncated Conical Thin Shell Structures. *J. of Sound and Vibration*, 150, (1991), 509-516.

Xu, C.S.; Xia, Z.Q.; Chia, C.Y.: Nonlinear Theory and Vibration Analysis of Laminated Truncated, Thick, Conical Shells. *Int. J. Non-Linear Mechanics* 31, (1996), 139-154.

Address: W. K. Chai, J. G. DeHaven, M. Hanson and H. S. Tzou, Department of Mechanical Engineering, Structronics Lab.University of Kentucky, Lexington, KY 40506-0503, U.S.A. V:(859)257-6336; F:(859)257-3304;
e-mail: hstzou@engr.uky.edu